International Journal of Pure and Applied Physics. ISSN 0973-1776 Volume 13, Number 1 (2017), pp. 238-243

Study of nuclear dynamics using IQMD model

Rajni Bansal

Department of Physics, MCM DAV College for Women, Sector 36 A, Chandigarh -160 036, India.

***Abstract*-We study the role of colliding geometry, incident energy as well as system mass in the nuclear dynamics. For the present analysis, we simulate the reactions of $^{15}C+^{15}C$, $^{48}Ca+^{48}Ca$ and $^{197}Au+^{197}Au$ at different incident energies ranging between 50 and 400 MeV/nucleon for central and peripheral collisions within the framework of Isospin-dependent Quantum Molecular Dynamics (IQMD) Model. Our study reveals significant sensitivity of the nuclear dynamics towards the various entrance channel parameters.**

I. INTRODUCTION

An extensive amount of research has been devoted to understand the nuclear matter at the extreme conditions of temperature and density. In this direction, collective transverse flow i.e., the space-momentum correlations of dynamic region, has been proved to be a powerful tool [1, 2]. For the past three decades, it has been used extensively to constrain nuclear equation of state (EOS) as well as in-medium nucleon-nucleon (nn) cross-section of the nuclear matter [3–5]. The dependence of collective transverse flow on various entrance channel parameters such as incident energy [3, 6–9], colliding geometry [3, 4, 10,11] as well as on the system mass [5, 12–14] is well established experimentally as well as theoretically. The energy dependence of collective transverse flow results in change in the sign of collective transverse flow, and hence led to its disappearance at a particular energy known as energy of vanishing flow (EVF). This happens because of the balancing
of attractive mean field (dominant at low energy) and repulsive nn scattering (dominant at high energy) at that particular energy. The energy of vanishing flow is of greater
significance because of its weak sensitivity towards various experimental uncertainties and has been measured for more than 15 systems [14]. Similarly, transverse flow decreases with impact parameter and this sensitivity to colliding geometry increases at high incident energies [3, 4]. Also the transverse in-plane flow increases with system mass which in
turn leads to a power law dependence of the energy of vanishing flow ($\propto A^{-\tau}$) [5, 14]. In recent times, with the advent of radioactive-ion beam (RIB) facilities, the role of isospin degree of freedom on transverse flow and its disappearance has been examined experientially [15, 16] as well as theoretically [11, 17, 18] by considering various isotopic as well as isobaric reactions. The effect of isospin degree of freedom on EVF is found to be much more pronounced at peripheral colliding geometries compared to central ones [11]. At the same time, we know that transverse flow originates from the density gradient formed during the compressional phase of a reaction and thus, is found to be closely related to the nuclear dynamics of a reaction. Therefore, it becomes important to explore the effects of various entrance channel parameters on the nuclear dynamics also. In this regard, Puri *et al.* [19] studied the behavior of nuclear dynamics governed by collision rate, density, anisotropy ratio and relative momentum with incident energy, system mass as well as colliding geometry using Relativistic Quantum Molecular Dynamics (RQMD) model. The study pointed towards the mass independent nature of temperature. Similarly, nuclear dynamics have also been investigated at energy of vanishing flow [20, 21] and peak centre-of-mass energy (energy corresponding to maximum fragment production) [22] using Quantum Molecular Dynamics (QMD) model. Recently, the role of isospin degree of freedom on nuclear dynamics for the reactions involving neutron rich colliding pairs is studied by Gautam *et al.* using Isospin-dependent Quantum Molecular Dynamics (IQMD) model [23, 24]. These studies were limited to central collisions only. Therefore, study of the behavior of nuclear dynamics towards the incident energy, system mass and colliding geometry for neutron rich system is still missing. With this in mind, here we
aim to study the effects of various entrance channel parameters on the nuclear dynamics such as density, collision rate, participant and spectator matter, anisotropy ratio as well as relative momentum using IQMD model.

II. THE MODEL

In IQMD model [25, 26], isospin degree of freedom enters into calculations via symmetry potential, cross-sections and Coulomb interaction. In this model, the nucleons are represented by the Gaussian-shaped density distributions and propagate under the Hamilton equations of motion with potential given by:

$$V^{ij}(r'-r) = V^{ij}_{Skyrme} + V^{ij}_{Yukawa} + V^{ij}_{Coul} + V^{ij}_{mdi} + V^{ij}_{sym}$$

$$= \left[t_1\, \delta(\vec{r}' - \vec{r}) + t_2\, \delta(\vec{r}' - \vec{r})\, \rho^{\gamma-1} \left(\frac{\vec{r}' + \vec{r}}{2} \right) \right]$$

$$+ t_3 \frac{\exp(-|(\vec{r}' - \vec{r})|/\mu)}{(|(\vec{r}' - \vec{r})|/\mu)} + \frac{Z_i Z_j e^2}{|(\vec{r}' - \vec{r})|}$$

$$+ t_4 \ln^2\left[t_5(\vec{p}' - \vec{p})^2 + 1\right]\delta(\vec{r}' - \vec{r})$$
$$+ t_6 \frac{1}{\rho_0} T_{3i} T_{3j} \delta(\vec{r}_i' - \vec{r}_j).$$

Here *Zi* and *Zj* denote the charges of i^{th} and j^{th} baryon, and T_{3i} and T_{3j} are their respective T_3 components (i.e., 1/2 for protons and −1/2 for neutrons). The parameters $t_1, \ldots, t_5$ are adjusted to the real part of the nucleonic optical potential. It is worth mentioning that IQMD model has been successfully used for the analysis of large number of observables from low to high incident energies [8, 11, 14, 23, 26].

A. Results and Discussion

For the present study, we simulate $^{15}C+^{15}C$, $^{48}Ca+^{48}Ca$ and $^{197}Au+^{197}Au$ the reactions of at incident energies of 50, 100, 200 and 400 MeV/nucleon for central (b_{red} = 0.25) and peripheral (b_{red} = 0.75) geometries. Here we use a soft EOS supplemented by momentum dependent interactions (MDI) along with 20% reduced cross-section to simulate the above reactions. The choice of above set has been advocated by many previous studies in the literature [11, 14, 26].

For the present study we uses $\langle p_x/A \rangle$ versus rapidity where the linear fit to the slope at mid rapidity region gives the reduced flow. Also we uses the quantity '*directed transverse momentum* $\langle p_x^{dir} \rangle$' which is defined as:

$$< P_x^{dir} >= \frac{1}{A}\sum_{i=1}^{A} sign\{Y_i\} p_z(i)$$

where $Y(i)$ is the rapidity and $p_x(i)$ is the transverse momentum of *ith* particle. In this definition, all rapidity bins are taken into account. It, therefore, presents an easier way of measuring the in-plane flow than complicated functions such as $\langle p_x/A \rangle$ plots. It is worth mentioning that both the methods gave similar results for the energy of vanishing flow [13]. Firstly we will see the behavior of transverse in-plane flow with entrance channel parameters so as to relate it with nuclear dynamics.

In Fig. 1, we display $\langle p_x/A \rangle$ as a function of $Y_{C.M.}/Y_{beam}$ at freeze out time (left panels) and $\langle p_x^{dir} \rangle$ as a function of reaction time (right panels). To see the role of incident energy on transverse flow, we display the reactions of $^{48}Ca+^{48}Ca$ for central collisions at incident energies ranging between 50 and 400 MeV/nucleon in top panels. The short-dashed, solid, short-dotted and short-dash-dotted lines represent the calculations performed at incident energies of 50, 100, 200 and 400 MeV/nucleon, respectively. We see that slope of $\langle p_x/A \rangle$ versus $Y_{C.M.}/Y_{beam}$ is negative at lower incident energy (50 MeV/nucleon) which turns positive at certain energy and becomes more sharp as one moves towards higher incident energies. This indicates that transverse flow increases with increase in the incident energy. Similar behavior of $\langle p_x^{dir} \rangle$ towards the incident energy is also observed from Fig 1(b). Here, it remains negative at 50 MeV/nucleon and becomes more and more positive with increase in the incident energy. This is because of the fact that at low incident energies the reaction dynamics is governed by the attractive part of the nuclear mean field causing the emission of particles in the backward angles, whereas at high incident energies repulsive nn scattering dominates and, hence, pushes the particles into the forward (positive) angles. Also the $\langle p_x^{dir} \rangle$ saturates much earlier for the reactions at high incident energies compared to the reactions at low incident energies indicating that the reaction finishes earlier in the former case. Next to investigate the system size effects on transverse flow, we display the reactions of $^{15}C+^{15}C$, $^{48}Ca+^{48}Ca$ and $^{197}Au+^{197}Au$ at an incident energy of 100 MeV/nucleon for central collisions in middle panels. Dotted, solid and dash-dotted lines correspond to the reactions of $^{15}C+^{15}C$, $^{48}Ca+^{48}Ca$ and $^{197}Au+^{197}Au$, respectively.

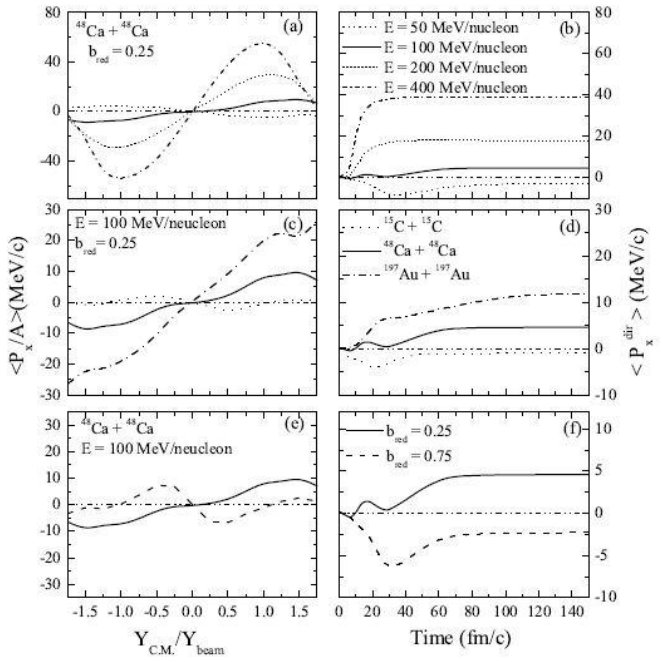

Fig. 1. Left and right panels correspond to $< p_x/A >$ as a function of $Y_{C.M.}/Y_{beam}$ at final time and the time evolution of $\langle p_x^{dir} \rangle$ respectively. Lines in the top, middle and bottom panels correspond to different colliding geometries, incident energies and system masses, respectively and are explained in the text

We see that slope of $\langle p_x/A \rangle$ is negative for the reaction of $^{15}C+^{15}C$ and becomes positive for the reactions of $^{48}Ca+^{48}Ca$ and $^{197}Au+^{197}Au$. It clearly shows that transverse flow increases with the mass of the system. Similar conclusions can be drawn from the time evolution of $\langle p_x^{dir} \rangle$ (Fig. 1(d)). We also notice that $\langle p_x^{dir} \rangle$ saturates much earlier for reaction involving lighter nuclei and saturation time increases with the mass of the system indicating that reaction finishes later in heavier system. Finally, we investigated the role of colliding geometry on the transverse flow, for reactions of $^{48}Ca+^{48}Ca$ at an incident energy of 100 MeV/nucleon (see bottom panels). The solid and dashed lines correspond to central and peripheral collisions, respectively. From the figure, we see

that the slope of $\langle p_x/A \rangle$ in mid rapidity zone is positive for the central collisions and becomes negative for peripheral collisions. Similar trend is also observed for $\langle p_x^{dir} \rangle$ as it is also positive (negative) for central (peripheral) collisions in agreement with earlier studies [3, 9].

Next, we investigate the role of entrance channel parameters on nuclear dynamics. In present approach, the matter density is calculated by [27]

$$f(r, p, t) = \sum_{i=1}^{A_p + A_T} \left(\frac{1}{2\pi L} \right)^{3/2} \exp(-(r - r_i(t))^2 / 2L)$$

Here A_T and AP stand, for the mass of the target and projectile, respectively. The density is calculated in a sphere of 2 fm. For details, reader is referred to Refs. [27]. First, we will see the influence of incident energy on nuclear dynamics.

For this analysis, in Fig. 2, we display the time evolution of maximum ($\langle \rho^{max} \rangle/\rho_0$) and average ($\langle \rho^{avg} \rangle/\rho_0$) density reached in the central sphere of radius around 2 fm, collision rate $\langle dN_{coll}/dt \rangle$, participant and spectator matter ($\langle Part/spect \rangle_{norm}$), anisotropy ratio ($\langle R_a \rangle$) as well as relative momentum ($\langle K_r \rangle$) for the reactions of $^{48}Ca+^{48}Ca$ and at incident energies of 50, 100, 200 and 400 MeV/nucleon represented by short dashed lines, solid, short-dotted and short-dash-dotted lines, respectively. From the figure, we see that nuclear density first rises as the reaction precedes, reaches a maxima during compressional phase and then starts decreasing during the freeze out. We also see the maximal value of average and maximum density increases with incident energy as expected. We also see that the maximum compression is achieved earlier for the reaction at high incident energies. Further in Fig. 2(c), we display the time evolution of collision rate at various incident energies. We see that collisions rate first increases with reaction time and after achieving maximum value during the compressional phase, it again start decreasing. Moreover the collisions rate also increases with incident energy. We also notice that $\langle dNcoll/dt \rangle$ does not change after 30 fm/c indicating that collisions happening after this stage does not alter the reaction dynamics. This is also evident from Fig. 1(b), where transverse momentum saturates at about 30 fm/c. Similar profile of the maximum/average density and collision rate with reaction time gives the evidences of the direct correlation of the collision rate and the nuclear density achieved in heavy ion collisions.

The another quantity which is directly related with the number of collisions is participant and spectator matter. The participant and spectator matter also has been proved to be a barometer for the energy of vanishing flow [21]. Here the participant matter is defined in terms of nucleonic concept, although there exist others definitions in terms of rapidity distribution etc. It is worth mentioning that all approaches lead to similar conclusions [21]. The nucleons which have suffered at least one collusion are called participant matter and the remaining nucleons are labelled as spectator matter. Note that here only those collisions are considered that are cleared by the Pauli principle.

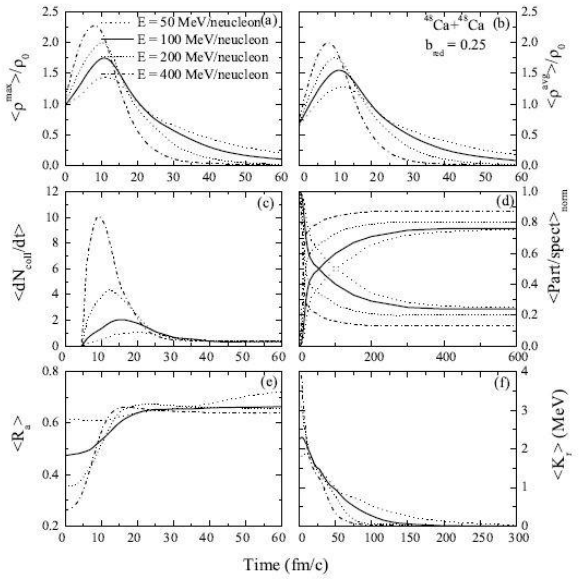

Fig. 2. The time evolution of maximal density (a), average density (b), collision rate (c), participant and spectator matter (d) anisotropy ratio (e) and relative momentum (f) for the reactions of $^{48}Ca+^{48}Ca$ at an incident energy 100 MeV/nucleon. Different lines correspond to different incident energies for the central collisions of $^{48}Ca+^{48}Ca$ as explained in the text.

Next, in Fig. 2(d) we display the time evolution of the normalized (with respect to total number of nucleons) participant and spectator matter. From the figure, we see that participant (spectator) matter increases (decreases) as the reaction proceeds. Also, the change of spectator matter into participant matter at high incident energies is more swift and sudden compared to lower incident energies. The saturation time of the participant/spectator matter increases with decrease in the incident energy. Also the participant matter present at the freeze out stage of a reaction increases with incident energy indicating the violence of the collisions at higher energies.

Thermalization is another aspect in the studies of heavy ion reactions. In the present case, the degree of equilibrium has been defined in two ways anisotropy ratio ($\langle R_a \rangle$) and relative momentum ($\langle K_r \rangle$). $\langle R_a \rangle$ is an indicator of global equilibrium and defined in Ref.[23,24].

It is worth mentioning that such a concept of local equilibrium is commonly used in the hydrodynamical model. Next in Figs. 2(e) & 2(f), we display the time evolution of anisotropy ratio and relative momentum, respectively. From Fig. 2(e), we see that $\langle R_a \rangle$ increases linearly with reaction time and finally saturates after the high dense phase ($\sim$ at 30 fm/c) is over indicating that collisions happening after that stage do not alter the equilibrium of the reaction. Also a lower $\langle R_a \rangle$ value is observed at the initial stage for the reaction at high incident

energies which increases with incident energy. This is because of the high longitudinal momentum (p_z) at higher energies. Also the maximum thermalization is achieved at lower incident energies (50MeV/nucleon). This clearly demonstrates the dominance of the mean field at lower energies (at the freeze out stage) which results in greater equilibrium. The decrease in the value of $\langle R_a \rangle$ with increase in incident energies indicates equally important role of mean field and nn scattering and hence this competition between the two does not let the better equilibrium to be achieved.

We also notice that after 100 MeV/nucleon, $\langle R_a \rangle$ is hardly affected by incident energy. Similar findings are reported in Ref. [28]. From Fig. 4(f), we see that relative momentum decreases as the reaction precedes and finally becomes zero at freeze out. Also initial value of $\langle K_r \rangle$ is more at higher incident energies (because of the greater relative momenta), as expected.

Next to investigate the system size effects on nuclear dynamics, in Fig. 3, we display all the above mentioned quantities for the reactions of $^{15}C+^{15}C$, $^{48}Ca+^{48}Ca$ and $^{197}Au+^{197}Au$ at an incident energy of 100 MeV/nucleon for central collisions. Dotted, solid and dash dotted lines represent the reactions of $^{15}C+^{15}C$, $^{48}Ca+^{48}Ca$ and $^{197}Au+^{197}Au$, respectively.

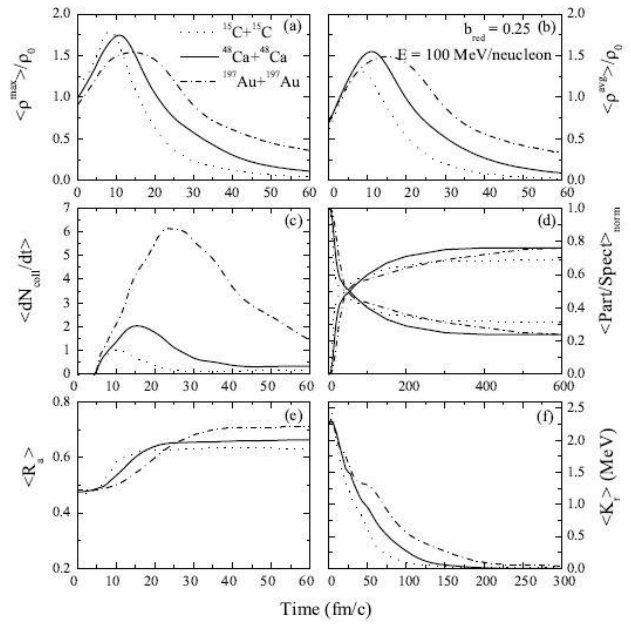

Fig. 3. Same as Fig. 2, but here different lines correspond to central collisions of different reactions as explained in the text.

From Fig. 3(a) (where the time evolution of density is plotted), we see that the reaction of $^{15}C+^{15}C$ leads to maximum compression (highest density) compared to medium ($^{48}Ca+^{48}Ca$) and heavy ($^{197}Au+^{197}Au$) mass systems. Also a wider density profile is observed in the reaction of heavy colliding nuclei indicating that interactions keeps on going in heavier systems for a longer time, hence reaction finishes later in heavier system as also inferred from Fig. 1(e), where the transverse flow for the reaction of $^{197}Au+^{197}Au$ saturates much later. The time at which maximum compression takes place gets delayed, as one moves from lighter to heavier system. We also notice that there is a substantial difference between the maximal value of maximal and average density in the case of $^{15}C+^{15}C$ collisions, representing non-homogeneous nature of dense matter in case of lighter systems. On the other hand, this difference between the maximal value of two densities disappears for the reactions of $^{48}Ca+^{48}Ca$ and $^{197}Au+^{197}Au$. This clearly demonstrates that dense matter is formed uniformly in the central region for the reaction involving heavier colliding nuclei. In Fig. 3(c), we display the collision rate as a function of time for the reactions of $^{15}C+^{15}C$, $^{48}Ca+^{48}Ca$ and $^{197}Au+^{197}Au$. We see that the reaction of $^{197}Au+^{197}Au$ leads to the highest collision rate. This is because of the greater number of participating nucleons in case of heavier system compared to lighter ones. We also find that collision rate profile is more wider for the reaction of $^{197}Au+^{197}Au$ compared to the reactions of $^{48}Ca+^{48}Ca$ and $^{15}C+^{15}C$. This is because of the larger interaction volume in the case of heavier system, therefore the interaction between nucleons continue for longer time and this, in turn, leads to a wider profile of collision rate. In Fig. 3(d), we display the time evolution of participant and spectator matter. We notice that change of spectator matter into the participant matter in lighter systems is more swift and sudden compared to medium and heavy mass system, where this change is slow and gradual. Also higher participant matter at the freeze out is observed for the reaction of $^{197}Au+^{197}Au$. This participant matter decreases as one moves towards lighter systems. It is worth mentioning that had these reactions simulated at their corresponding energies of vanishing flow, they must have been resulted in same participant matter [21]. In Fig. 3(e), we see that, anisotropy ratio first increases and then saturates with time. Now the initial value of $\langle R_a \rangle$ is same for all reactions because of the same incident energy (100 MeV/neucleon) in all the three cases. Also $\langle R_a \rangle$ saturates much later for the reaction of $^{197}Au+^{197}Au$ because of the fact that high dense phase exists for a longer time in case of heavier systems. We also notice that anisotropy ratio increases with system mass indicating that better thermalization is achieved in the reactions involving heavier colliding nuclei. Similar behavior is observed in case of relative momentum $\langle K_r \rangle$ also (see Fig. 3(f)).

Finally, we investigate the role of colliding geometry on the nuclear dynamics. In Fig. 4, we display time evolution of maximal and average density, collision rate , participant and spectator matter, anisotropy ratio as well as relative momentum for the reactions of $^{48}Ca+^{48}Ca$ at an incident energy of 100 MeV/neucleon at central (b_{red} = 0.25) and peripheral (b_{red} = 0.75) collisions, represented by solid and dashed lines, respectively.

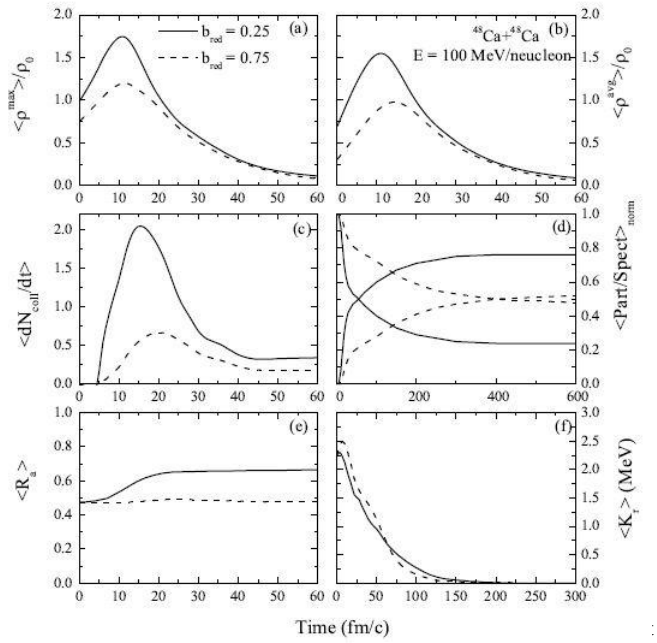

colliding geometries as explained in the text.

From the figure, we notice that central collisions lead to more compression compared to peripheral collisions, where the density achieved in the compressional zone remains almost equals to the normal nuclear matter density. Also the maximum value of nuclear density for central and peripheral collisions is attained at the same time in agreement with the predictions of the QMD model [19, 27]. In addition, the decrease of density with colliding geometry gives the signatures of the reduction in the transverse flow as when one moves from central to peripheral collisions (see Fig. 1(a) & (b)). From Fig. 4(c), we see that collision rate first increases with time, reaches a maximum at around 20-40 fm/c (which is the high dense phase of a reaction), and then finally decreases and becomes constant at around 80 fm/c. Here we find that collision rate decreases significantly, when one moves from central to peripheral geometry. This is because of less participant zone available in the peripheral collisions. Next, we display the time evolution of the participant and spectator matter in Fig. 4(d). From Fig. 4(d), we notice that the peripheral collisions result in lesser participant matter at the final stage of a reaction compared to central ones. Next the time evolution of anisotropy ratio ($\langle R_a \rangle$) and relative momentum ($\langle K_r \rangle$) are displayed in Figs. 4(e) & 4(f), respectively. We notice that for central collisions (solid line), $\langle R_a \rangle$ increases with time and then saturates at 15-30 fm/c, in contrary to peripheral collisions (dashed line) where it remains almost constant with time. Also in the central collision, the $\langle R_a \rangle$ value saturates as soon as the high density phase is over indicating that only the violent collisions happening during high dense phase of a reaction changes the momentum space significantly. Also the value of $\langle R_a \rangle$ is higher for central collisions compared to peripheral collisions, demonstrating that central collisions lead to better thermalization compared to peripheral ones as reported earlier in Ref. [19]. It is worth mentioning that neither central nor peripheral collisions result in the global equilibrium as the value of $\langle R_a \rangle$ always remains less than one. On the other hand, $\langle K_r \rangle$ shown in Fig. 4(f) decrease with the time for both central as well as peripheral collisions. This is because of the fact that with passage of time, density in central sphere decreases, and results in decrease in $\langle K_r \rangle$.

III. Conclusion

We investigated the role of various entrance channel parameters such as incident energy, system mass and colliding geometry on the nuclear dynamics via density, collision rate, participant/spectator matter, anisotropy ratio as well as relative momentum within the framework of IQMD model. Our study revealed the significant sensitivity of nuclear dynamics towards the entrance channel parameters. Also the collision rate and nuclear density are found to exhibit similar behavior towards the incident energy, colliding geometry as well as the system mass. Our study also pointed towards the better tendency of the heavier and central collisions for the equilibrium. Also collisions at low incident energy take significant time to develop the equilibrium because of the dominance of the mean field which keeps the nucleons together. The participant matter present at the final stages of a reaction is found to increase with incident energy as well as with the size of colliding nuclei.

Acknowledgment

Rajni Bansal is thankful to Prof. Rajeev K. Puri, Dept. Of Physics, Panjab University Chandigarh for the fruitful discussions.

References

[1] W. Scheid, H. M¨uller and W. Greiner. (1974, April). *Nuclear Shock Waves in Heavy-Ion Collisions.* Phys. Rev. Lett. 32 (13), PP. 741-745.

[2] H. A. Gustafsson et al. (1984, April). Collective Flow Observed in Relativistic Nuclear Collisions. Phys. Rev. Lett. 52 (18), PP. 1590-1593.

[3] G. F. Bertsch, W. G. Lynch and M. B. Tsang. (1984, May). Transverse momentum distributions in intermediate-energy heavy-ion collisions. Phys. Lett. B 189 (4), 384 -387.

[4] H. Zhou, Z. Li and Y. Zhou, Comm. Theor. Phys. 19, 199 (1993).

[5] G. D. Westfall et al. (1993,Sept.). Mass dependence of the disappearance of flow in nuclear collisions Phys. Rev. Lett. 71(13), PP. 1986- 1989.

[6] J. Lukasik et al**.** (2005, Feb.). Directed and elliptic flow in ^{197}Au + ^{197}Au at intermediate energies. Phys. Lett. B 608(3), PP. 223-230.

[7] A. Andronic et al. (2003, March). Directed flow in Au+Au, Xe+CsI, and Ni+Ni collisions and the nuclear equation of state. Phys. Rev. C 67(3), PP. 034907-19.

[8] A. D. Sood, R. K. Puri. (2006, Dec.). Influence of momentum dependent interaction on balance energy and mass dependence.Eur. Phys. J. A 30(3),PP. 571-577.

[9] S. Kumar and R. K. Puri. (1998,Nov.). Stability of fragments formed in the simulations of central heavy ion collisions.Phys. Rev. C 58(5), PP.2858-2863.

[10] D. J. Magestro et al. (2000, Jan).Disappearance of transverse flow in Au+Au collisions.Phys. Rev. C 61(2), PP.021602-4(R).

[11] S. Gautam, R. Chugh, A. D. Sood, R. K. Puri, C. Hartnack and J. Aichelin. (2010,June). Isospin effects on the energy of vanishing flow in heavy-ion collisions. J. Phys. G: Nucl. Part. Phys. 37(8), PP.085102-9.

[12] C. Guo et al. (2012,Feb.). Influence of symmetry energy on the balance enrgy of directed flow.Sci. Chin. Phys. Mech. Astr. 55(2), PP.252-259.

[13] A. D. Sood, R. K. Puri and J. Aichelin,. (2004, Aug.).Study of balance energy in central collisions for heavier nucleiPhys. Lett. B 594(3-4), PP.260-264.

[14] R. Bansal, S. Gautam and R. K. Puri. (2014, Feb).Systematic study of the energy of vanishing flow using IQMD model and comparison with various theoretical models. J. Phys. G: Nucl. Part. Phys. 41(3),PP. 035103-11.

[15] R. Pak et al. (1997). Isospin Dependence of Collective Transverse Flow in Nuclear Collisions. Phys. Rev. Lett. 78(6), PP.1022-1025.

[16] R. Pak et al. (1997). Isospin Dependence of the Balance Energy. Phys. Rev. Lett. 78(6), PP. 1026-1029

[17] B. A. Li et al. (1996, June). Isospin Dependence of Collective Flow in Heavy-Ion Collisions at Intermediate Energies. Phys. Rev. Lett. 76 (24), 4492-4495.

[18] L. W. Chen, F. S. Zhang and G. M Jin. (1998, Oct.). Analysis of isospin dependence of nuclear collective flow in an isospin-dependent quantum molecular dynamics model. Phys. Rev. C 58(4), PP.2283- 2291.

[19] R. K. Puri et al., (1994). Study of non-equilibirium effects and thermal properties of heavy ion collisions using a covalent approach. J. Phys. G: Nucl. Part. Phys. 20(11), PP.1817.

[20] A. D. Sood and R. K. Puri. (2004,Sept.). Nuclear dynamics at the balance energy. Phys. Rev. C 70(3), PP. 034611-7

[21] A. D. Sood and R. K. Puri. (2009,June). Participant-spectator matter at the energy of vanishing flow. Phys. Rev. C 79(6), PP. 064618-5

[22] S. Kaur and A. D. Sood, Pram. J. Phys. 76, 909 (2011).

[23] S. Gautam. (2011,June). Density and temperature of neutron-rich systems at the energy of vanishing flow in heavy-ion collisions. Phys. Rev. C 83(6),PP.064604-6.

[24] S. Gautam, and R. K. Puri.(2012,June).Participant-spectator matter and thermalization of neutron-rich systems at the energy of vanishing flow. Phys. Rev. C 85(6), PP. 067601-4.

[25] C. Hartnack et al.(1998,Feb.). Modelling the many-body dynamics of heavy ion collisions: Present status and future perspective. Eur. Phys. J. A 1(2), PP.151-159.

[26] R. Bansal, S. Gautam, R. K. Puri and J. Aichelin.(2015, Jan.). On the mass dependence of energy of vanishing flow for superheavy mass region.Eur. Phys. J. A 51, PP.2-7 .

[27] D. T. Khoa et al. (1992, June). Microscopic study of thermal properties of the nuclear matter formed in heavy-ion collisions. Nucl. Phys. A 542(4), PP. 671-698.

[28] Y. K. Vermani and M. Kaur. (2010, Sept.).Remarks on the non-equilibrium effects and collision dynamics in heavy-ion collisions. Phy. Scr. 82, PP.045202-6.